Sensing and Bio-Sensing Research 9 (2016) 38–44

Contents lists available at ScienceDirect

Sensing and Bio-Sensing Research

journal homepage: www.elsevier.com/locate/sbsr

Mechanical polishing as an improved surface treatment for platinum screen-printed electrodes

Junqiao Lee, Damien W.M. Arrigan, Debbie S. Silvester *

Nanochemistry Research Institute, Department of Chemistry, Curtin University, GPOBox U1987, Perth, Western, 6845, Australia

ARTICLE INFO

Article history:
Received 23 March 2016
Received in revised form 18 May 2016
Accepted 18 May 2016

Keywords:
Screen-printed electrodes
Polishing
Platinum
Activation
Pre-treatment
Cyclic voltammetry

ABSTRACT

The viability of mechanical polishing as a surface pre-treatment method for commercially available platinum screen-printed electrodes (SPEs) was investigated and compared to a range of other pre-treatment methods (UV-Ozone treatment, soaking in *N*,*N*-dimethylformamide, soaking and anodizing in aqueous NaOH solution, and ultrasonication in tetrahydrofuran). Conventional electrochemical activation of platinum SPEs in 0.5 M H_2SO_4 solution was ineffective for the removal of contaminants found to be passivating the screen-printed surfaces. However, mechanical polishing showed a significant improvement in hydrogen adsorption and in electrochemically active surface areas (probed by two different redox couples) due to the effective removal of surface contaminants. Results are also presented that suggest that SPEs are highly susceptible to degradation by strong acidic or caustic solutions, and could potentially lead to instability in long-term applications due to continual etching of the binding materials. The ability of SPEs to be polished effectively extends the reusability of these traditionally "single-use" devices.

1. Introduction

Although various commercial brands of screen-printed electrodes (SPEs) are now available, the specific compositions of the materials used in their manufacture are often not disclosed. Screen-printing inks typically comprise of a blend of conductive material, polymeric binders and suitable solvents [1,2]. These "electrochemically-inert" binding materials can potentially block the electrochemically active surfaces, resulting in slower kinetics for heterogeneous reactions [2,3]. As a result, the development of surface treatment methods to enhance the electrochemical properties of SPEs has been of great interest [2]. In our previous work, the compatibility of room temperature ionic liquids (RTILs) with various commercial SPEs has been investigated for the sensing of ammonia [4], chlorine [5], methylamine and hydrogen chloride [6] and oxygen [7] gases. It was discovered that SPEs gave a poorer response for oxygen reduction (compared to conventional disk electrodes), and that a cross-over of the forward and reverse scans was present in cyclic voltammograms recorded in imidazolium based RTILs [7]. It was proposed that this was due to a chemical reaction of the highly reactive superoxide with the binding materials present on these electrodes [7]. This demonstrates that the binding materials in SPEs could in fact undesirably interfere with the electrochemistry of certain target species.

Investigations into pre-treatment methods for SPEs have been largely focused on carbon (C) based SPEs [2,3,8–10], mainly due to their low cost and wide use in a range of sensing strategies. However results from our earlier work [7] showed that C-SPEs do not perform as well as metal-based SPEs (e.g. silver (Ag), gold (Au), and platinum (Pt)) when used with RTIL solvents. Platinum SPEs (Pt-SPEs), on the other hand, showed the best response out of the four SPEs investigated. This has motivated us to investigate alternative pre-treatment methods for Pt-SPEs in order to improve their long-term stability for gas-sensing applications [7].

This paper explores the viability of mechanical polishing as an alternative pre-treatment for Pt-SPEs. To the best of our knowledge, there are only two reports of polishing of SPEs (both carbon). Office paper was used to polish C-SPEs, showing improved responses for IgG antibody adsorption and sensing [10], and alumina slurry or diamond spray was used to polish C-SPEs on polishing cloths, showing an improved analytical performance for the sensing of nitrite [11]. These techniques can be considered more "gentle" compared to the mechanical polishing with a machine polisher used in the present work. Four additional pre-treatment methods were explored as a comparison, two of which were reported to be ideal for C-SPEs, namely soaking in *N*,*N*-dimethylformamide (DMF) [8], and soaking followed by anodizing in aqueous NaOH solution [2], one (UV-Ozone treatment) was chosen as a similar method to oxygen plasma treatment (previously suggested for C-SPEs) [9], and one (ultrasonication in THF) to serve as a control to the polishing procedure investigated. It is to be noted that these treatments when applied to SPEs will not necessarily lead to a "cleaner"

* Corresponding author.
E-mail address: d.silvester-dean@curtin.edu.au (D.S. Silvester).

http://dx.doi.org/10.1016/j.sbsr.2016.05.006

surface ideal for electrochemical experiments. The goal is to assess the viability of the different pre-treatment methods for Pt-SPEs and the possibility of using mechanical polishing of SPEs in a similar way to the well-known polishing of metal disk electrodes.

2. Materials and methods

2.1. Chemicals and materials

Ultrapure water (resistivity of 18.2 MΩ cm) prepared by an ultrapure laboratory water purification system (Millipore Pty Ltd., North Ryde, NSW, Australia), and ethanol (EtOH 99%, Sigma-Aldrich Pty Ltd., NSW, Australia) were used as solvents to rinse the Pt-SPEs (DropSens DRP-550, Oviedo, Spain) before and after experiments. Tetrahydrofuran (THF > 99%, Sigma-Aldrich Pty Ltd., NSW, Australia) and *N*,*N*-Dimethylformamide (DMF 99.8%, Sigma-Aldrich Pty Ltd., NSW, Australia) were used as received without purification. 0.5 M and 3 M Sodium hydroxide (NaOH, ≥98%, Sigma-Aldrich Pty Ltd., NSW, Australia), 0.5 M sulfuric acid ($H_2SO_{4(aq)}$, 95–98 wt.%, Ajax Finechem, WA, Australia), and 0.1 M potassium chloride (KCl, >99.5%, Fluka, Buchs, Switzerland) aqueous (aq) solutions were prepared using ultrapure water. 1.1 mM hexaammineruthenium(III) chloride ($[Ru(NH_3)_6]Cl_3$, 98%, Sigma-Aldrich Pty Ltd., NSW, Australia), and 1.0 mM potassium hexacyanoferrate(III) ($K_3[Fe(CN)_6]$, 99 + %, Strem Chemicals, Massachusetts, USA) in electrolyte solution of 0.1 M KCl were used to characterize the electrochemically active surface areas of the Pt-SPEs.

2.2. Treatment methods for Pt-SPEs

2.2.1. Mechanical polishing

The Pt-SPEs used in this study contain a blue polymer mask to cover the underlying Ag traces (Fig. 1 (top)). The blue mask is made of a synthetic polymeric dielectric material that is soluble in THF. Accordingly, the electrode was sonicated in THF then polished with a mechanical polisher (Dap-V, Struers, Copenhagen, Denmark) at a rotation speed of 600 rpm, using 1 μm alumina powder (Kemet Australia Pty Ltd., Marayong, NSW) on a soft lapping pad (Buehler, Illionis, USA) until a glossy finish was obtained (see Fig. 1 (bottom)). The planar electrode was pressed down firmly on the rotating polishing pad for approximately 1 min while moving the electrode in a circular motion, in order to ensure even polishing of electrodes. This is believed to be a much "harsher" method of polishing compared to that used previously for a C-SPE [10]. It was noted that for C-SPEs, polishing with emery paper easily destroyed the SPE [10], but the destruction of Pt-SPEs was not observed in the present work, despite the harsh polishing method employed. The exposed screen-printed Ag electrical traces were then re-masked with SELLEYS® Silicone Sealant (100% Silicone, purchased from local hardware store) to leave only the three electrode surfaces uncovered. Photographs of unpolished and silicone-masked polished Pt-SPEs with connecting wires soldered on are shown in Fig. 1. A more detailed account of the polishing protocol followed can be found in Section A of the Supporting information (SI).

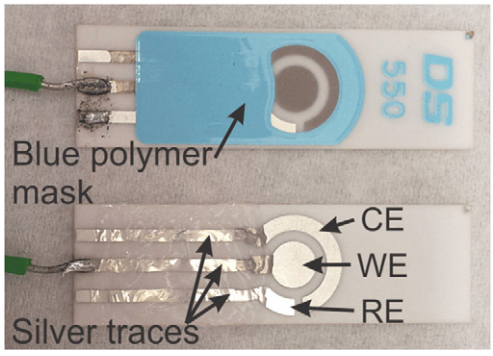

Fig. 1. (Top) fresh-out-of-the-box (untreated), and (bottom) mechanically polished Pt-SPEs (ca. 1 min duration on a mechanical polisher at a rotation speed of 600 rpm). A layer of silicone mask was applied to cover the exposed screen-printed silver traces. Wires were soldered at the end of the working electrode trace to connect the working electrode with the potentiostat.

2.2.2. Other treatment methods

Due to the unavailability of a plasma cleaner, a 50 W UV-ozone cleaner (BIOFORCE Nanosciences, Inc., Model: UV.TC.220 USA) was employed (Section B in SI), and Pt-SPEs were exposed for 30 mins. NaOH treated Pt-SPEs were prepared based on a method used for C-SPEs [2]; Pt-SPEs were soaked in 3 M $NaOH_{(aq)}$ for 1 h, then anodized at 1.2 V vs. Ag/AgCl in 0.5 $NaOH_{(aq)}$ for 20 s. The NaOH treated Pt-SPEs were then thoroughly rinsed in ultrapure water, and dried under a stream of nitrogen gas. DMF treated Pt-SPEs were prepared based on the pre-treatment method suggested for C-SPEs [8]. Pt-SPEs were briefly soaked in DMF in a small glass vial for 5 mins, before being cured in an oven for 20 mins at 100 °C in a covered glass Petri dish. Pt-SPEs designated as "THF treated" were subjected to the same pre-washing and post-washing methods (by sonication in THF and other solvents) as polished Pt-SPEs, but with the mechanical polishing step omitted. The THF treated Pt-SPE serves as a control for the polished Pt-SPEs, and also to explore its viability as a "stand-alone" alternative pre-treatment method for Pt-SPEs.

2.3. Electrochemical experiments

Electrochemical experiments were performed using a μ-Autolab Type III potentiostat (Eco-Chemie, Netherlands) interfaced to a PC with NOVA 1.8 software. All experiments were carried out inside a custom made aluminum Faraday cage and at a temperature of 293 ± 2 K. A copper wire was soldered at the end of the middle Ag trace to allow the working electrode of the Pt-SPE to be connected to the potentiostat (see Fig. 1). The Pt-SPE has a nominal working electrode diameter of 4 mm, with the working (WE) and counter (CE) electrodes made of screen-printed Pt, and with a screen-printed Ag quasi-reference electrode (RE). The CE and RE on the SPE were not used in the experiments; instead, an external reference electrode (Ag|AgCl|KCl (1.0 M)) (BASi, Indiana, USA), and CE (Pt wire, Ø = 0.50 mm, Goodfellow Cambridge Ltd., UK) coil were used. This was to ensure that any differences observed in the voltammetric response were purely attributed to differences in the condition of the WEs. The Pt wire CE was cleaned by rinsing in EtOH, flaming in a Bunsen burner, sonicating in EtOH and then in ultrapure water.

Before measurements, solutions were purged with nitrogen gas by bubbling for 15 mins. Cyclic voltammograms (CVs) were collected at scan rates of 100 mV s^{-1} or 1 V s^{-1}, and a step potential of 3 mV. For the $[Ru(NH_3)_6]^{3+/2+}$ and $[Fe(CN)_6]^{3-/4-}$ redox experiments, background corrections of the peak currents, I_p, were performed. This was carried out by subtracting the linearly extrapolated current (from the non-Faradaic part of the CV just before onset of the peak) from I_p. Potential-step chronoamperometry (PSCA) measurements were performed for 20 s (with 60 s pre-biasing at 0 V) with suitable over-potentials to ensure fast kinetics for convergence to a Cottrellian type response. PSCA in 0.1 M $KCl_{(aq)}$ was also performed to allow for background-subtraction of the PSCA data. Finally, electrochemical impedance spectroscopy (EIS) of the unpolished and polished Pt-SPEs was conducted in 0.1 M $KCl_{(aq)}$ electrolyte solution. EIS data was measured in the frequency range 1 mHz–1.5 MHz, operating in the single-sine-wave mode, with an RMS AC voltage of 5 mV oscillating about the open-circuit-potential (OCP) on the WE. For EIS experiments, to ensure that the RE was as close to the WE as possible, the Ag-RE on the integrated Pt-SPE device was used. A Pt coil CE was employed.

The electrochemically active surface areas were derived from background-corrected CV peak currents for each Pt-SPE via the Randles-Sevčik equation [12,13],

$$i_p = \left(2.69 \times 10^5\right) n^{\frac{3}{2}} A D^{\frac{1}{2}} \nu^{\frac{1}{2}} c \quad (1)$$

and from the diffusion limited currents via chronoamperometric experiments using the Cottrell equation [14],

$$i_d = \frac{n F A D^{1/2} c}{\pi^{1/2} t^{1/2}} \quad (2)$$

where n is the number of electrons transferred per molecule, F is Faraday's constant, A is the area of the electrode, D is the diffusion coefficient, ν is the scan rate, t is the time, and c is the concentration of the redox species. D for $[Ru(NH_3)_6]^{3+}$ and $[Fe(CN)_6]^{3-}$ in 0.1 M $KCl_{(aq)}$ are 8.43 ($\pm$0.03) $\times 10^{-10}$ m^2 s^{-1} [15] and 7.20 ($\pm$0.18) $\times 10^{-10}$ m^2 s^{-1} [16] at 298 K, respectively.

2.4. Imaging experiments

Scanning electron microscopy (SEM, Zeiss Evo 40XVP model) was performed on the working WE of SPEs, and confocal optical imaging and Raman mapping were performed using a WITec (alpha300 series) confocal Raman microscope (for more details, see Section C and D respectively in the Supporting information).

3. Results and discussion

To investigate the effectiveness of mechanical polishing on Pt-SPEs, both hydrogen adsorption/desorption voltammetry and cyclic voltammetry of the $[Fe(CN)_6]^{3-/4-}$ and $[Ru(NH_3)_6]^{3+/2+}$ redox couples were performed. Four additional pre-treatment methods, namely sonication in THF, UV-ozone treatment, NaOH treatment, and DMF soaking were also investigated. Topographical surface areas of unpolished and polished SPEs were estimated from their 3D confocal optical stacked images. The following sections provide a qualitative comparison of the efficacy of each of the pre-treatment methods studied.

3.1. Voltammetry in 0.5 M $H_2SO_{4(aq)}$

Hydrogen adsorption/desorption voltammetry is commonly used for the activation of Pt surfaces as well as the estimation of electrochemically active surface areas [17–21]. Adsorption/desorption of hydrogen on platinum surfaces is described by the following equation [17]:

$$H^+_{(aq)} + e^- \rightleftharpoons H_{adsorbed} \quad (3)$$

CV experiments on six Pt-SPEs (one untreated and 5 subject to different pre-treatment methods) were conducted by repeated cycling between +1.25 V and −0.3 V in 0.5 M $H_2SO_{4(aq)}$, with the starting potential set at the open-circuit potential (OCP). Fig. 2 compares the voltammograms of the 25th and 150th consecutive scans. The redox process at ca. 1 V (oxidative), and at 0.46 V (reductive) correspond to the oxidation and reduction of Pt via the formation of quasi-3D platinum oxide lattices [18,22,23]. Broad contaminant shoulders between 0.6 V and 0.9 V on the oxidative scans appear to vary between differently-treated SPEs. A large contaminant peak at 0.42 V on the oxidative scan (which grows with progressive CV cycles) was present in all CVs with the exception of NaOH treated SPEs. This peak was substantially decreased for the polished SPE (Fig. 2b). The hydrogen adsorption and desorption peaks (at ca. −0.1 V) were considerably larger for both polished (Fig. 2b) and NaOH treated (Fig. 2e) Pt-SPEs compared to the unpolished (Fig. 2a) Pt-SPEs. A pair of reversible contaminant peaks, at 0 V for reduction, and 0.23 V for oxidation (which diminished with progressive CV cycles) was more obvious for the untreated (Fig. 2a) and polished (Fig. 2b) SPEs. These contaminant peaks are believed to be primarily due to the presence of polymer binders exposed on the screen-printed surfaces [2,8–10].

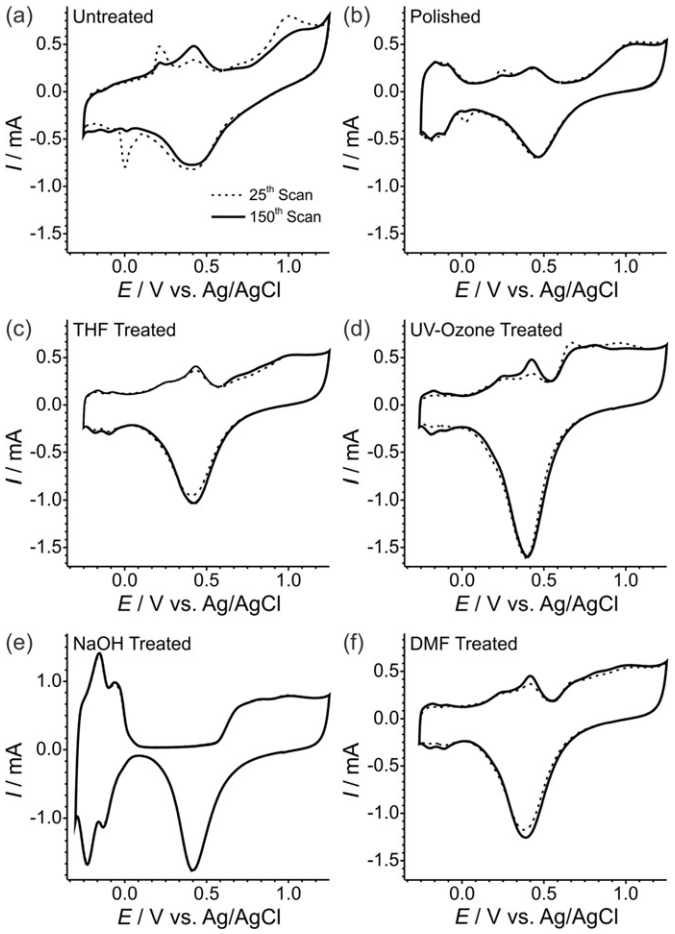

Fig. 2. The 25th (- -) and 150th (–) cyclic voltammetric cycles of 0.5 M $H_2SO_{4(aq)}$, scanned between 1.25 V and −0.3 V at 1 V s^{-1} (with starting potential set as the OCP) on untreated and the various treated Pt-SPEs. Voltammograms are plotted on the same current scale to allow for direct comparison, except for the NaOH treated SPE due to its substantially larger $H^+_{(aq)}$ desorption waves. The solid line overlays the dashed line exactly where the latter is not visible.

Peaks relating to the oxidation and reduction of Pt stabilized within the first 10–15 cycles for all Pt-SPEs, while characteristic hydrogen adsorption and desorption peaks gradually become more distinct as the CV cycles progressed. This can be attributed to the gradual desorption of passivating contaminants (e.g. SPE binding materials) with each CV cycle, leading to an increase in active sites for hydrogen adsorption. Hydrogen adsorption/desorption peaks for untreated Pt-SPEs remained negligible, even after 200 cycles (see Fig. 2a). Continuing past 500 cycles did not further increase hydrogen adsorption/desorption currents for any of the SPEs. Polished (Fig. 2b) and NaOH treated (Fig. 2e) Pt-SPEs showed a substantial increase in the hydrogen desorption peak currents compared to the other treated SPEs, and stability was generally achieved within ca. 25 cycles. These results revealed that repeated CV cycling in 0.5 M $H_2SO_{4(aq)}$ was ineffective in removing the passivating layer of surface contaminant that was clearly present, whereas polishing and the NaOH treatment appeared to be highly effective. While the NaOH treatment "appears" to be the most effective (based on the largest hydrogen adsorption peaks in the CVs in H_2SO_4), the voltammetric responses of two common redox couples (see next section) were far from ideal, suggesting that the SPE paste is unstable in the presence of NaOH (discussed later in section 3.4).

3.2. Cyclic voltammetry of $[Ru(NH_3)_6]^{3+}$ and $[Fe(CN)_6]^{3-}$ on Pt-SPEs

Untreated and treated Pt-SPEs were characterized in aqueous $[Ru(NH_3)_6]Cl_3$ and $K_3[Fe(CN)_6]$ solutions with both CV and PSCA. CVs for 1.1 mM $[Ru(NH_3)_6]Cl_3$ and 1.0 mM $K_3[Fe(CN)_6]$ in 0.1 M $KCl_{(aq)}$ are presented in Figs. 3 and 4, respectively. The peak-to-peak separations for the two redox couples, ΔE_p are presented in Table 1.

The redox reactions are: [24]

$$[Ru(NH_3)_6]^{3+} + e^- \rightleftharpoons [Ru(NH_3)_6]^{2+} \quad (4)$$

$$[Fe(CN)_6]^{3-} + e^- \rightleftharpoons [Fe(CN)_6]^{4-} \quad (5)$$

For $[Ru(NH_3)_6]^{3+/2+}$, ΔE_p for untreated, polished, NaOH and UV-ozone treated SPEs were all 76 mV, while the DMF treated SPE (Fig. 3f) shows a significant improvement in electron transfer kinetics with a ΔE_p of 64 mV. A pre-peak is present in all the CVs except for the polished Pt-SPE. ΔE_p for the THF treated SPE (Fig. 3c) was slightly higher at 79 mV, and the CV exhibited signs of surface contamination (at ca. −0.3 V in the anodic scan). Comparing the CVs of $[Fe(CN)_6]^{3-/4-}$, the THF treated SPE (Fig. 4c) also showed larger ΔE_p compared to untreated SPE (Fig. 4a). However the shape of the voltammetry appears to remain unaffected by the THF treatment. Significantly larger capacitive currents were observed for NaOH treated SPEs in both $[Ru(NH_3)_6]^{3+/2+}$ and

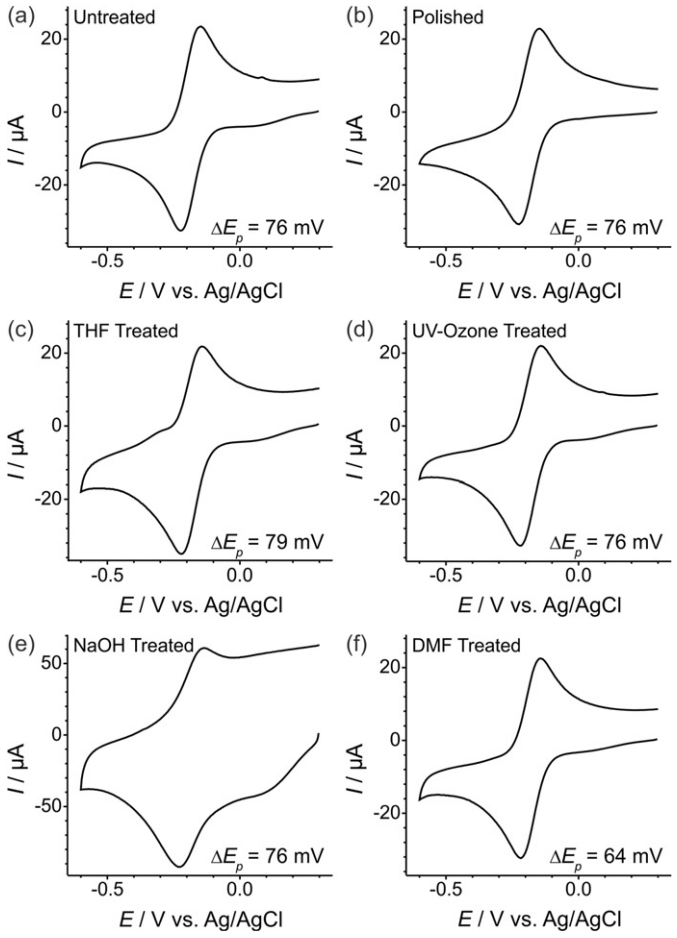

Fig. 3. Cyclic voltammetry of 1.1 mM of $[Ru(NH_3)_6]Cl_3$ in 0.1 M $KCl_{(aq)}$ supporting electrolyte, scanned between 0.3 V and −0.6 V at 100 mV s^{-1}, on untreated and various treated Pt-SPEs. All the voltammograms were plotted on the same current scale to allow for direct comparison, except for the NaOH treated SPE due to its substantially larger currents.

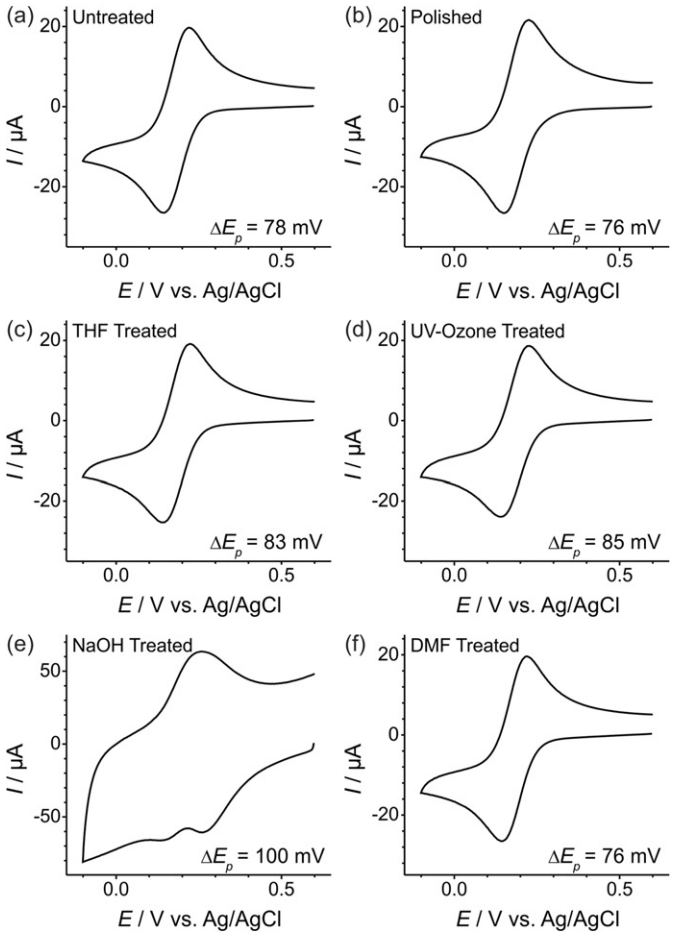

Fig. 4. Cyclic voltammetry of 1.0 mM of $[Ru(NH_3)_6]Cl_3$ in 0.1 M $KCl_{(aq)}$ supporting electrolyte, scanned between 0.3 V and −0.6 V at 100 mV s^{-1}, on untreated and various treated Pt-SPEs. All the voltammograms were plotted on the same current scale to allow for direct comparison, except for the NaOH treated SPE due to its substantially larger currents.

$[Fe(CN)_6]^{3-/4-}$ CVs (Figs. 3e and 4e), and the possible reasons for this are discussed later.

$[Fe(CN)_6]^{3-}$ is known to possess a weak inner sphere electron transfer character [25], and can be catalysed by the Pt surface to form a passivating layer of Prussian blue ($KFe(II)[Fe(III)(CN)_6]$) [26]. A larger variability in ΔE_p (and E_p-$E_{p½}$) for $[Fe(CN)_6]^{3-/4-}$ experiments was observed (compared to $[Ru(NH_3)_6]^{3+/2+}$ experiments) indicating that while the pre-treatment methods do not significantly affect the kinetics of purely outer sphere electron transfer reactions (e.g. $[Ru(NH_3)_6]^{3+/2+}$), the $[Fe(CN)_6]^{3-/4-}$ CVs appear to be more sensitive to the condition of the electrode surface. For instance, although the ΔE_p of $[Ru(NH_3)_6]^{3+/2+}$ on UV-ozone treated Pt-SPE (Fig. 3d) was the same as an untreated Pt-SPE (Fig. 3a) at 76 mV, $[Fe(CN)_6]^{3-/4-}$ the UV-ozone treated Pt-SPE (Fig. 4d) showed a significantly wider ΔE_p at 85 mV compared to the untreated Pt-SPE (78 mV, Fig. 4a).

For the NaOH treated SPE, two reduction peaks were present (Fig. 4e). The cathodic peak at ca. −150 mV occurs at a potential more negative than the $[Ru(NH_3)_6]^{2+}$ oxidation peak, thus it was attributed to $[Ru(NH_3)_6]^{3+}$ reduction. The cause of the appearance of the other peak at −261 mV after the NaOH pre-treatment is unclear at present. However, ΔE_p for $[Ru(NH_3)_6]^{3+/2+}$ on NaOH treated SPE (Fig. 3e) appears to be unaffected (compared to untreated SPEs), while a much wider ΔE_p was observed for $[Fe(CN)_6]^{3-/4-}$ (Fig. 4e). Significant and visible deterioration of the structural integrity of Pt-SPEs after NaOH pre-treatment was also observed (Section F in SI). The non-typical CVs

Table 1
Background corrected reduction peak currents, I_p, peak-to-peak separations, ΔE_p, and electrochemically active surface area, A_e, of Pt-SPEs subjected to different treatment protocols, obtained from CV and PSCA of $[Ru(NH_3)_6]^{3+/2+}$ redox couple (Fig. 3), and of $[Fe(CN)_6]^{3-/4-}$ redox couple (Fig. 4). A_e normalized with respect to the topographic surface area, A_t (from Table 2), were also derived.

		$[Ru(NH_3)_6]^{3+/2+}$				$[Fe(CN)_6]^{3-/4-}$			
Method	Treatment	I_p/μA	ΔE_p/mV	A_e/mm^2	A_e/A_t	I_p/μA	ΔE_p/mV	A_e/mm^2	A_e/A_t
CV	Untreated	26.7	76	10.3	0.32	25.1	78	11.0	0.34
	Polished	26.2	76	10.1	0.42	25.3	76	11.1	0.46
	THF-sonication	28.2	79	10.9	0.34	23.5	83	10.3	0.32
	UV-ozone	26.7	76	10.3	0.32	22.4	85	9.80	0.30
	NaOH	32.9	76	12.7	0.39	n/a	100	n/a	n/a
	DMF	26.2	64	10.1	0.31	10.9	76	10.9	0.34
PSCA	Untreated	n/a	n/a	11.6	0.36	n/a	n/a	10.9	0.34
	Polished	n/a	n/a	11.7	0.48	n/a	n/a	11.9	0.49
	THF-sonication	n/a	n/a	10.5	0.33	n/a	n/a	8.37	0.26
	UV-ozone	n/a	n/a	9.18	0.28	n/a	n/a	10.4	0.32
	NaOH	n/a	n/a	15.1	0.47	n/a	n/a	n/a	n/a
	DMF	n/a	n/a	11.0	0.34	n/a	n/a	8.13	0.25

of NaOH treated Pt-SPEs with these two redox couples, combined with physical signs of degradation, raise doubts on the suitability of NaOH treatment for SPEs. The results from the mechanically polished and DMF treated Pt-SPEs appear to show the most promise.

3.3. Estimation of topographical surface areas

SEM images of unpolished and polished WEs of Pt-SPEs are presented in Fig. 5. The electrode was polished on a mechanical polisher at a rotation speed of 600 rpm for ca. 1 min. The images show that the untreated Pt-SPE surface is extremely rough with ridges, but that the microscopic topographical features are significantly flattened after polishing. The expected reduction in topographical surface area, A_t, of polished Pt-SPEs was characterized using 3D confocal optical imaging. Details of the instrument and methods used to collect the 3D-stacked confocal optical images are given in Section D of the SI. Some topographical features were inaccessible or hidden to optical imaging due to the rough nature of the surfaces. Thus, the topographical surface areas are expected to be underestimated (especially for the rougher surface of the untreated Pt-SPE). The manufacturer states a WE geometric surface area, A_g, of 12.6 mm^2 (i.e. 4.0 mm diameter) for Pt-SPEs. The ratio of A_t to A_g of the WE (i.e. A_t/A_g, also known as the "rugosity" of a surface [22,23]) is presented in Table 2. For a perfectly flat and smooth surface, A_t/A_g would be unity. The uncertainties, estimated as half of the range of values from two duplicate measurements, show good agreement for A_t (i.e. 5.8% and 8.3%, respectively, for the untreated and polished Pt-SPEs). The larger uncertainty for the polished SPEs could be due to variation with their preparation (e.g. force applied, position of the SPE on the rotating polishing pad, etc.) even when subjected to a similar duration of mechanical polishing. The optical microscope images of Pt-SPEs treated by the other protocols showed no differences compared to the untreated Pt-SPEs (up to a magnification of 60×).

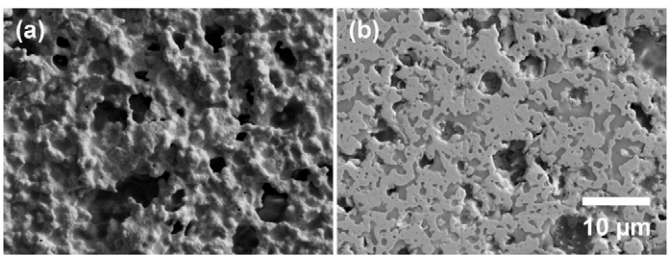

Fig. 5. SEM images of representative (a) unpolished and (b) polished Pt-SPEs. The width the images represent 50 μm on the SPE (see Section C of the Supporting information for the instrumentation parameters used).

3.4. Comparison of active surface area vs. topographical surface area

The electrochemically active surface area for hydrogen adsorption, A_e, (Table 3) was estimated from the hydrogen adsorption/desorption CVs (Fig. 2) on the 25th cycle using a standard method [17] (Section G in the SI). The hydrogen desorption peak on the untreated Pt-SPE (Fig. 2) could not be reliably analysed and was omitted. Polished Pt-SPEs show an order of magnitude increase in surface area accessible for hydrogen adsorption compared to the THF-treated Pt-SPE (which also served as the control sample for the polished Pt-SPEs). A_e/A_t provides a measure of the amount of electrochemically active sites with respect to the topographic surface area, and should be unity for a uniformly electrochemically active surface. A_e/A_t for the UV-ozone and DMF treated Pt-SPEs were not significantly larger than the THF-treated Pt-SPE. A_e/A_t of the NaOH treated Pt-SPE (at 4.06) showed a large increase, which may be incorrectly interpreted as having achieved exceptional "cleaning", relative to the other pre-treatments investigated. However, this value is well over the theoretical maximum of unity and is indicative of substantial over-etching of the Pt-SPE by the 3 M $NaOH_{(aq)}$ solution (illustrated in Fig. 6). The weakening of the supporting polymeric binders holding the conductive Pt particles together (Fig. E.1 in SI) may compromise the structural integrity of the screen-printed material (as discussed in Section F in SI). This could also substantially increase the capacitance in the CVs (as observed in Figs. 3 and 4), due to severe degradation in the quality of the electrical contacts along the electrical percolation channels setup by the Pt particles.

A_e for untreated and treated Pt-SPEs were also derived from CVs of 1.1 mM $[Ru(NH_3)_6]Cl_3$ and 1.0 mM $[Fe(CN)_6]^{3-}$ in 0.1 M $KCl_{(aq)}$ (Figs. 3 and 4) using Eq. (1), and from PSCA experiments using Eq. (2). The results obtained from the two electrochemical probes are summarised in Table 1. The reduction peak current for $[Fe(CN)_6]^{3-}$ on the NaOH treated Pt-SPE could not be reliably analysed, and PSCA could not be reliably conducted (see Fig. 4) and are therefore omitted from Table 1. Firstly, it is interesting to also observe that A_e/A_t of the polished and NaOH treated Pt-SPEs (Table 1) did not increase as drastically as the respective data obtained from the hydrogen adsorption/desorption experiments (Table 3). This indicates that the different electrochemical probe species provide different information on the untreated and various treated Pt-SPE surfaces, and

Table 2
Topographic surface area, A_t, (estimated from 3D confocal optical stacked images) and the ratio between A_t and the geometric surface area, A_g, of unpolished and polished Pt-SPEs.

Treatment	Surface Area, A_t/mm^2	A_t/A_g
Untreated	32.3 ± 1.9	2.57 ± 0.15
Polished	24.2 ± 2.0	1.93 ± 0.16

Table 3
Electrochemically active surface area, A_e, of Pt-SPEs subjected to different treatment protocols, obtained from hydrogen desorption voltammetries conducted in 0.5 M $H_2SO_{4(aq)}$ (presented in Fig. 2), and A_e normalized with respect to the topographic surface area, A_t (from Table 3).

Treatment	A_e/mm^2	A_e/A_t
Untreated	n/a	n/a
Polished	18.2	0.75
THF-sonication	1.89	0.06
UV-ozone	2.72	0.08
NaOH	131*	4.06
DMF	1.80	0.06

* Note that although the apparent A_e of NaOH treated SPEs appears to be the largest (i.e. could be considered the "cleanest" surface), this is clearly not the case due to the non-ideal voltammetry exhibited in Figs. 3e and 4e.

can be explained by the fact that A_e/A_t in Tables 1 and 3 were derived from markedly different electrochemical processes – namely hydrogen adsorption/desorption vs. $[Ru(NH_3)_6]^{3+/2+}$ and $[Fe(CN)_6]^{3-/4-}$ redox couples. For instance, part of the surfaces of the unpolished Pt-SPEs (even those subjected to various non-polishing treatments) may remain substantially blocked by a thin coating of residual contaminants, preventing hydrogen adsorption. However, the outer sphere electron transfer of the $[Ru(NH_3)_6]^{3+/2+}$ redox process [24] remains largely unaffected by regions more "thinly" contaminated at the surface. In contrast, $[Fe(CN)_6]^{3-/4-}$, which exhibits a more inner sphere character [27], is more strongly affected, resulting in a larger ΔE_p (Table 1) and the absence of additional minor peaks (e.g. observed in Fig. 3 for $[Ru(NH_3)_6]^{3+/2+}$, but absent in Fig. 4 for $[Fe(CN)_6]^{3-/4-}$) that may correspond to the redox reaction occurring on the contaminated surfaces. Notably in Fig. 3, only the CV for the polished Pt-SPE shows an absence of these additional minor peaks, which may also be indicative of an electrochemically "cleaner" surface. Diffusion of the larger $[Ru(NH_3)_6]^{3+}$ and $[Fe(CN)_6]^{3-}$ ions (compared to H^+) may not be able to effectively characterize microscopic gaps that may be present between the tightly packed Pt particles, due to etching of binding materials during NaOH exposure, as illustrated in Fig. 6. This may explain the discrepancy in A_e/A_t obtained from the hydrogen adsorption CV (Table 3), and from the $[Ru(NH_3)_6]^{3+}$ and $[Fe(CN)_6]^{3-}$ CVs (Table 1).

From Table 1, it can be seen that A_e/A_t (from both $[Ru(NH_3)_6]^{3+/2+}$ and $[Fe(CN)_6]^{3-/4-}$ CVs) was improved after polishing compared to all the other Pt-SPEs. Polishing appears to be the only pre-treatment method that gives a significant increase in the hydrogen adsorption active surface area, without deterioration of the structural integrity of the

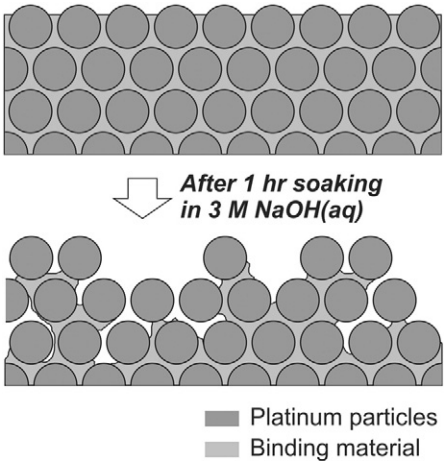

Fig. 6. Cartoon illustrating the possible effect of the harsh NaOH treatment of platinum screen-printed electrodes. The Pt-SPEs were soaked in concentrated 3 M NaOH for 1 h.

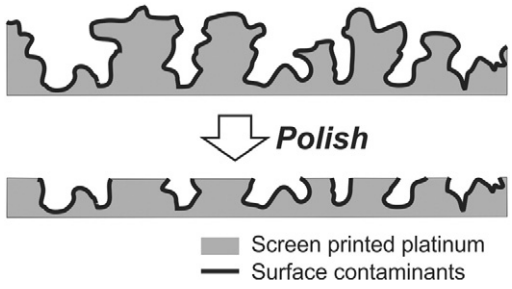

Fig. 7. Illustration of a screen-printed platinum surface before (top) and after (bottom) being subjected to mechanical polishing.

screen-printed material, as happens in the case of NaOH treatment where large capacitive currents were observed (Figs. 3e and 4e). Fig. 7 illustrates the removal of surface contaminants (such as excess binding materials or adsorbed organic oils, etc., probably from the manufacturing and packaging process) by mechanical polishing, while exposing a fresh surface of screen-printed Pt material.

Although the binding materials in Pt-SPEs were found to be susceptible to acid attack (Section F in SI), it is unlikely that the increase in A_e/A_t was due to immersion in the 0.5 M $H_2SO_{4(aq)}$ solution. Firstly, the duration (<30 mins) for which the SPEs were immersed in the more dilute acid solution was not sufficient to cause substantial structural deterioration of the screen-printed material (Section F in SI). Furthermore, an increase in the active sites for hydrogen adsorption was apparent from the initial voltammetric scan, and stability was typically established within the first 25 cycles. Most importantly, the other treated/untreated SPEs did not exhibit any signs of improvement, even well beyond the 150th CV cycle in 0.5 M $H_2SO_{4(aq)}$. Comparing the results of Pt-SPEs subjected to the various pre-treatment methods, polishing provides the best improvement in A_e/A_t and its $[Ru(NH_3)_6]^{3+/2+}$ CV shape (disappearance of a pre-peak that was present in all the other CVs). Finally, different SPEs (i.e. Au, Ag, and C), exposed to acidic and alkaline solutions for >1 h were also found to structurally degrade (Section F in SI). This could lead to instability due to the continual etching of binding materials, especially for long-term (>1 h) experiments in aqueous acidic or alkaline solutions using these SPEs.

3.5. Electrochemical impedance spectroscopy

For a qualitative verification of the impact of polishing, electrochemical impedance spectroscopy (EIS) was performed on unpolished and polished Pt-SPEs (Fig. 8). Large and distinct time constants were

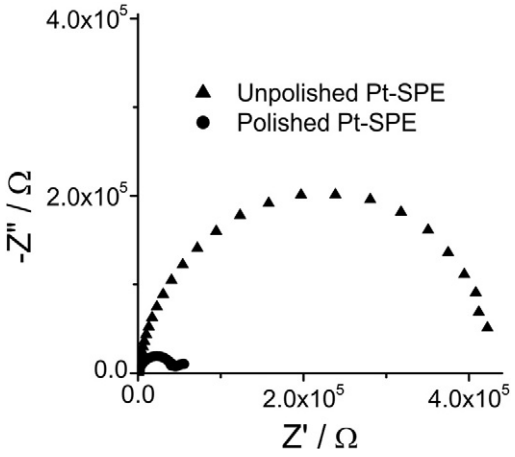

Fig. 8. Nyquist plot of (▲) unpolished and (●) polished Pt-SPEs, collected in the frequency range of 1 mHz to 1.5 MHz (single-sine-wave mode) at RMS AC voltage of 5 mV oscillating about the OCP, in 0.1 M $KCl_{(aq)}$.

observed in the Nyquist plots for unpolished Pt-SPEs. Polishing, however, resulted in a substantial decrease of the time constant polarization resistance, by a factor of ca. 10. This suggests the presence of a dielectric film (e.g. binding material) present on the unpolished Pt-SPE, which is substantially reduced after polishing. The presence of surface contaminants on unpolished Pt-SPE surfaces was further verified via confocal Raman mapping (Fig. D.1 and Section D in SI).

4. Conclusions

Mechanical polishing as a surface pre-treatment method for Pt-SPEs was explored and compared to other pre-treatments. Mechanical polishing showed a superior performance, as determined by hydrogen adsorption/desorption currents and electrochemically active surface areas, caused by the effective removal of the surface contaminants. Of the other pre-treatment methods, activation of Pt-SPEs in 0.5 M $H_2SO_{4(aq)}$ was discovered to be ineffective for the removal of contaminants which substantially passivated the screen-printed surfaces to hydrogen adsorption. NaOH treatment of Pt-SPEs showed an impressive enhancement in the active hydrogen adsorption surface area. However, large capacitive background currents in the $[Ru(NH_3)_6]^{3+/2+}$ and $[Fe(CN)_6]^{3-/4-}$ CVs were observed, likely due to over-etching. Tests conducted on different SPEs suggest that they are susceptible to degradation in strong acidic or caustic solutions. A marked improvement in the $[Ru(NH_3)_6]^{3+/2+}$ redox couple kinetics after DMF treatment was also observed.

Mechanical polishing as a pre-treatment method can potentially also be extended to Ag-SPEs and Au-SPEs, provided that the counter and reference electrodes of those devices are made of screen-printed materials that can withstand the harsh mechanical polishing investigated in this work. Mechanical polishing is a facile standard surface pre-treatment method for the preparation of electrodes for electrochemical use. It is cheap and convenient to employ, and does not require expensive specialized instruments (such as a plasma or UV-ozone cleaner) nor the use of organic solvents such as DMF or highly corrosive NaOH. Most importantly, it may enable the re-utilization of "fouled" surfaces, thus extending the life of these traditionally "single-use" devices. The benefits of mechanical polishing of Pt-SPEs have recently been demonstrated by our group, which shows the achievement of prolonged oxygen detection in ionic liquids [28].

Acknowledgements

DSS thanks the Australian Research Council for a Discovery Early Career Researcher Award (DECRA: DE120101456). JL thanks Curtin University for PhD funding through an Australian Postgraduate Award (APA) and Curtin Research Scholarship (CRS). The authors acknowledge the use of Curtin University's Microscopy & Microanalysis Facility, whose instrumentation has been partially funded by the University, State and Commonwealth Governments, and the use of the instruments of the Scanning Probe Microscopy facility of the Nanochemistry Research Institute/Department of Chemistry at Curtin University, funded by ARC LIEF grant number LE130100121.

Appendix A. Supplementary data

Experimental details on the polishing procedure and other treatment methods, SEM imaging, confocal imaging and Raman mapping, AFM imaging, details on the degradation of SPEs exposed to acid, and details on the calculation of the hydrogen adsorption surface area. Supplementary data to this article can be found online at http://dx.doi.org/10.1016/j.sbsr.2016.05.006.

References

[1] P. Fanjul-Bolado, D. Hernández-Santos, P.J. Lamas-Ardisana, A. Martín-Pernía, A. Costa-García, Electrochemical characterization of screen-printed and conventional carbon paste electrodes, Electrochim. Acta 53 (2008) 3635–3642.
[2] H. Wei, J.-J. Sun, Y. Xie, C.-G. Lin, Y.-M. Wang, W.-H. Yin, G.-N. Chen, Enhanced electrochemical performance at screen-printed carbon electrodes by a new pretreating procedure, Anal. Chim. Acta 588 (2007) 297–303.
[3] R.O. Kadara, N. Jenkinson, C.E. Banks, Characterisation of commercially available electrochemical sensing platforms, Sensors Actuators B 138 (2009) 556–562.
[4] K. Murugappan, J. Lee, D.S. Silvester, Comparative study of screen printed electrodes for ammonia gas sensing in ionic liquids, Electrochem. Commun. 13 (2011) 1435–1438.
[5] K. Murugappan, D.W.M. Arrigan, D.S. Silvester, Electrochemical behavior of chlorine on platinum microdisk and screen-printed electrodes in a room temperature ionic liquid, J. Phys. Chem. C 119 (2015) 23572–23579.
[6] K. Murugappan, D.S. Silvester, Sensors for highly toxic gases: methylamine and hydrogen chloride detection at low concentrations in an ionic liquid on Pt screen printed electrodes, Sensors 15 (2015) 26866–26876.
[7] J. Lee, K. Murugappan, D.W.M. Arrigan, D.S. Silvester, Oxygen reduction voltammetry on platinum macrodisk and screen-printed electrodes in ionic liquids: reaction of the electrogenerated superoxide species with compounds used in the paste of Pt screen-printed electrodes? Electrochim. Acta 101 (2013) 158–168.
[8] A.P. Washe, P. Lozano-Sanchez, D. Bejarano-Nosas, I. Katakis, Facile and versatile approaches to enhancing electrochemical performance of screen printed electrodes, Electrochim. Acta 91 (2013) 166–172.
[9] S.C. Wang, K.S. Chang, C.J. Yuan, Enhancement of electrochemical properties of screen-printed carbon electrodes by oxygen plasma treatment, Electrochim. Acta 54 (2009) 4937–4943.
[10] M. Pravda, C. O'Meara, G.G. Guilbault, Polishing of Screen-Printed Electrodes Improves IgG Talanta, 54 (2001) 887–892.
[11] L.R. Cumba, C.W. Foster, D.A.C. Brownson, J.P. Smith, J. Iniesta, Can the Mechanical Activation (polishing) of Screen-Printed Electrodes Enhance their Electroanalytical Response? Analyst 141 (2016) 2791–2799.
[12] J.E.B. Randles, Kinetics of rapid electrode reactions, Discuss. Faraday Soc. 1 (1947) 11–19.
[13] A. Sevcik, Oscillographic polarography with periodical triangular voltage, Collect. Czechoslov. Chem. Commun. 13 (1948) 349–377.
[14] F.F. Cottrell, The cut off current in galvanic polarisation, considered as a diffusion problem, Z. Phys. Chem. 42 (1903) 385–431.
[15] Y. Wang, J.G. Limon-Petersen, R.G. Compton, Measurement of the diffusion coefficients of $[Ru(NH_3)_6]^{3+}$ and $[Ru(NH_3)_6]^{2+}$ in aqueous solution using microelectrode double potential step chronoamperometry, J. Electroanal. Chem. 652 (2011) 13–17.
[16] S.J. Konopka, B. McDuffie, Diffusion coefficients of ferri- and ferrocyanide ions in aqueous media, using twin-electrode thin-layer electrochemistry, Anal. Chem. 42 (1970) 1741–1746.
[17] Bio-Logic Science Instruments, Calculation of the platinum's Active Surface, Application Note #11 (Retrieved from Www.Bio-Logic.Info), (2013) 1–3.
[18] G. Jerkiewicz, G. Vatankhah, J. Lessard, M.P. Soriaga, Y.-S. Park, Surface-oxide growth at platinum electrodes in aqueous H_2SO_4. Reexamination of its mechanism through combined cyclic-voltammetry, electrochemical quartz-crystal nanobalance, and Auger electron spectroscopy measurements, Electrochim. Acta 49 (2004) 1451–1459.
[19] M. Chatenet, M. Aurousseau, R. Durand, F. Andolfatto, Silver-platinum bimetallic catalysis for oxygen cathodes in chlor-alkali electrolysis. Comparison with pure platinum, J. Electrochem. Soc. 150 (2003) D47–D55.
[20] D.C. Rodger, W. Li, J.D. Weiland, M.S. Humayun, Y.-C. Tai, Flexible Circuit Technologies for Biomedical Applications, Chapter 1., Advances in Micro/Nano Electromechanical Systems and Fabrication Technologies (2013) 25.
[21] M.A.G. Zevenbergen, D. Wouters, V.-A.T. Dam, S.H. Brongersma, M. Crego-Calama, Electrochemical sensing of ethylene employing a thin ionic-liquid layer (supporting info), Anal. Chem. 83 (2011) 6300–6307.
[22] H. Angerstein-Kozlowska, B.E. Conway, W.B.A. Sharp, The real condition of electrochemically oxidized platinum surfaces: part I. Resolution of component processes, J. Electroanal. Chem. Interfacial Electrochem. 43 (1973) 9–36.
[23] B.E. Conway, Electrochemical oxide film formation at noble metals as a surface-chemical process, Prog. Surf. Sci. 49 (1995) 331–452.
[24] J. Blumberger, M. Sprik, Ab initio molecular dynamics simulation of the aqueous Ru^{2+}/Ru^{3+} redox reaction: the Marcus perspective, J. Phys. Chem. B 109 (2005) 6793–6804.
[25] J.K. Mbadcam, G.F.T. Wouaha, V.H. Gomdje, Adsorption of ferricyanide ion on activated carbon and γ-alumina, *E*-J. Chem. 7 (2010) 721–726.
[26] M.C. Granger, G.M. Swain, The influence of surface interactions on the reversibility of ferri/ferrocyanide at boron-doped diamond thin-film electrodes, J. Electrochem. Soc. 146 (1999) 4551–4558.
[27] C.H. An Wong, A. Ambrosi, M. Pumera, Thermally reduced graphenes exhibiting a close relationship to amorphous carbon, Nanoscale 4 (2012) 4972–4977.
[28] J. Lee, D.W.M. Arrigan, D.S. Silvester, Achievement of prolonged oxygen detection in room-temperature ionic liquids on mechanically polished platinum screen-printed electrodes, Anal. Chem. 88 (2016) 5104–5111.